


# Graphene oxide-based nanofluidic membranes for reverse electro dialysis that generate electricity from salinity gradients

Changchun Yu<sup>1,2</sup> | Yiming Xiang<sup>3</sup> | Tom Lawson<sup>4</sup> | Yandi Zhou<sup>1,2</sup> |  
Pingan Song<sup>5</sup> | Shulei Chou<sup>6</sup> | Yong Liu<sup>1,2</sup> 

<sup>1</sup>School of Ophthalmology and Optometry/School of Biomedical Engineering, Wenzhou Medical University, Wenzhou, Zhejiang, China

<sup>2</sup>National Engineering Research Centre for Ophthalmology and Optometry, Eye Hospital, Wenzhou Medical University, China

<sup>3</sup>School of Energy, Quanzhou Vocational and Technical University, Quanzhou, Fujian, China

<sup>4</sup>School of Chemical Engineering, University of New South Wales, Sydney, New South Wales, Australia

<sup>5</sup>School of Agriculture and Environmental Science, Centre for Future Materials, University of Southern Queensland, Springfield, Queensland, Australia

<sup>6</sup>Institute for Carbon Neutralization, College of Chemistry and Materials Engineering, Wenzhou University, Wenzhou, Zhejiang, China

## Correspondence

Shulei Chou, Institute for Carbon Neutralization, College of Chemistry and Materials Engineering, Wenzhou University, Wenzhou University Town, Wenzhou, Zhejiang 325035, China.  
Email: [chou@wzu.edu.cn](mailto:chou@wzu.edu.cn)

Yong Liu, School of Ophthalmology and Optometry/School of Biomedical Engineering, Wenzhou Medical University, 270 Xueyuanxi Rd, Wenzhou, Zhejiang 325027, China.  
Email: [yongliu@wmu.edu.cn](mailto:yongliu@wmu.edu.cn)

## Funding information

Key Research and Development Program of Zhejiang Province, Grant/Award Number: 2021C04019; National Natural Science Foundation of China, Grant/Award Number: U20A20338; Natural Science Foundation of Zhejiang Province, Grant/Award Number: LQ21H180012

## Abstract

A widely employed energy technology, known as reverse electro dialysis (RED), holds the promise of delivering clean and renewable electricity from water. This technology involves the interaction of two or more bodies of water with varying concentrations of salt ions. The movement of these ions across a membrane generates electricity. However, the efficiency of these systems faces a challenge due to membrane performance degradation over time, often caused by channel blockages. One potential solution to enhance system efficiency is the use of nanofluidic membranes. These specialized membranes offer high ion exchange capacity, abundant ion sources, and customizable channels with varying sizes and properties. Graphene oxide (GO)-based membranes have emerged as particularly promising candidates in this regard, garnering significant attention in recent literature. This work provides a comprehensive overview of the literature surrounding GO membranes and their applications in RED systems. It also highlights recent advancements in the utilization of GO membranes within these systems. Finally, it explores the potential of these membranes to play a pivotal role in electricity generation within RED systems.

## KEYWORDS

graphene oxide, ion gradients, nanofluidic membranes, reverse electro dialysis, salinity gradient power

This is an open access article under the terms of the [Creative Commons Attribution](https://creativecommons.org/licenses/by/4.0/) License, which permits use, distribution and reproduction in any medium, provided the original work is properly cited.

© 2024 The Authors. *Carbon Energy* published by Wenzhou University and John Wiley & Sons Australia, Ltd.

## 1 | INTRODUCTION

Salinity gradient power holds the promise of generating clean and sustainable energy from water sources.<sup>1</sup> This innovative approach involves a water conservancy system that could potentially replace fossil fuels. It operates by allowing two mixed aqueous solutions with varying salinities to pass through a membrane using a process known as pressure-retarded osmosis and reverse electrodialysis (RED), ultimately creating an electric potential.<sup>2</sup> Pressure-retarded osmosis enables water to cross the membrane while impeding the transport of salt. RED, in turn, directly converts chemical potential energy into electricity by employing an anion-exchange membrane (AEM) and cation-exchange membrane (CEM) and a reverse desalination process.<sup>3</sup> The process generates useful work from salinity gradients by forming a repeating unit consisting of a CEM, a high concentration (HC) compartment, an AEM, and a low concentration (LC) compartment. In this setup, the selective movement of anions and cations from the HC solution across the AEM and CEM, respectively, to the LC chambers creates a net charged ion flux. Typically, titanium mesh electrodes serve as the anode and cathode, facilitating current measurements. Cations and anions from high salinity streams traverse the CEM and AEM in opposite directions along their respective concentration gradients, and this ionic flow can be converted into electricity through redox reactions occurring on the electrodes.

The primary challenge in creating an efficient RED-based system lies in obtaining suitable ion-exchange membranes (IEMs).<sup>4</sup> These systems cannot function effectively without membranes that possess efficient permselectivity (the permeability ratio of ions),<sup>5</sup> durability (the ability to maintain integrity),<sup>6</sup> antifouling features (the ability to prevent attachment of unwanted organisms),<sup>7</sup> and cost-effectiveness.<sup>8</sup> The transmembrane electrical potential serves as the driving force behind ion flux, and ion channels respond to electric fields, enabling communication and signaling among permeable ionic species.

Two crucial factors influencing the electrical potential for power density in the RED system are permselectivity and ion conductivity.<sup>9</sup> These factors present a trade-off relationship in IEMs. Researchers often use permselectivity-conductivity plots to assess performance.<sup>10</sup> Permselectivity refers to the ability of IEMs to selectively transport counterions while excluding co-ions. The theoretical electromotive force ( $E_{\text{emf}}$ ) can be calculated using the Nernst equation<sup>11</sup>

$$E_{\text{emf}} = N_m \alpha RT / zF \ln(\gamma_{\text{HS}} C_{\text{HS}} / \gamma_{\text{LS}} C_{\text{LS}}), \quad (1)$$

in which  $N_m$  is the number of IEMs,  $\alpha$  is the average membrane permselectivity,  $F$  is the Faraday constant

(96,485 C mol<sup>-1</sup>), and  $z$  is the ionic valence (1 for Na<sup>+</sup> and Cl<sup>-</sup>). A higher permselectivity increases the voltage output according to this equation.<sup>12</sup> The RED system effectively functions as a dialytic battery, with ionic resistance (or ion conductivity) reflecting the internal resistance of the battery. Redox reactions at the electrodes convert the net current from selective ion transport into usable electricity while maintaining electroneutrality. The ionic resistance affects the system's energy efficiency and power output, and achieving both high permselectivity and high conductivity remains a challenge.<sup>13</sup>

Recent developments in RED membrane materials include nanomaterials with unique ionic exchange properties, such as metal-organic frameworks (MOFs),<sup>14</sup> ceramics,<sup>15</sup> and carbon-based materials. Even though MOFs and ceramics are widely investigated for the RED application, they are expensive to make on a large scale.<sup>16</sup> Among these, carbon nanomaterials, particularly two-dimensional (2D) graphene-based materials, have garnered significant attention for use in RED membranes.<sup>17</sup> They offer three main advantages. First, their atomically thin structure allows graphene membranes with nanometer-sized pores to achieve high permeability and selectivity. The 2D graphene plane improves ionic transfer and enhances overall membrane functionality.<sup>18</sup> Second, graphene oxide (GO), the oxidized form of graphene, effectively sieves ions and molecules due to its abundant negatively charged groups, such as hydroxyl, carbonyl, and carboxyl. Third, the stacked interlayer channels of GO enable scalable membrane production via filtration methods or shear-induced fabrication, providing a significant advantage over the limited scalability of nanopore structures in single-layer 2D materials.<sup>19</sup> Consequently, GO-based nanofluidic diodes with synthetic nanopores and nanochannels present high-performance options for RED membranes. Over the past 5 years, numerous researchers have explored GO-based composites as potential RED membranes, as detailed in Figure 1.<sup>20</sup>

However, further exploration is essential to advance experimental approaches and deepening the fundamental understanding of GO for salinity power generation. Previous reviews have predominantly concentrated on high-performance nanofluidic membranes for large-scale salinity gradient energy conversion<sup>3</sup> and 2D materials to enhance osmotic energy harvesting.<sup>21</sup> This work focuses exclusively on GO and its composites, which are the most typical 2D nanomaterials known for their rich surface functional groups and ease of processing. Specifically, we outline the roles and benefits of GO-based RED membranes in salinity power generation and provide insights into future developments and applications that could facilitate practical use and boost salinity power generation.

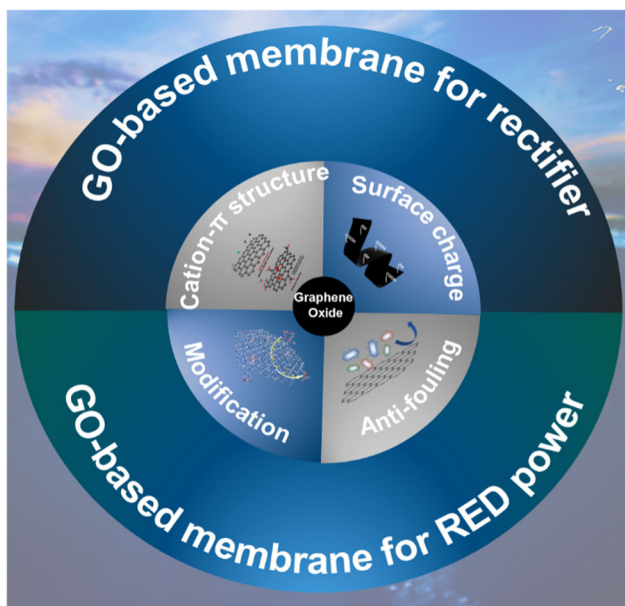


**FIGURE 1** An outline summary of the GO-based RED membrane that can be used for different salinity power generation systems. The picture in the lower left quarter was reproduced with permission: Copyright 2016, Wiley-VCH.<sup>20</sup>

## 2 | FUNCTIONALIZATION OF GO MEMBRANES FOR RED

GO is a 2D flat sheet that is covalently linked by aromatic domains ( $sp^2$  clusters)<sup>22</sup> and various oxygen functionalities (such as hydroxyl, epoxy, carboxyl, and carbonyl/hydroxyl functional groups). The cross-linked effect by cation- $\pi$  interactions enables GO to reorganize ions in a unique way. The GO membrane organizes ions locally into an alternatively ordered structure in an aqueous solution. This can generate various values of currents in different anion solutions. This occurs because of the unique inner structure of GO, that is, the oxygen-containing functional groups on the basal plane and edges that result in small  $sp^2$  regions isolated with the  $sp^3$  oxidized matrix.<sup>23</sup> This kind of structure benefits the ionic recognition of GO sheets. The coordination with  $sp^3$  carbons occurs between the transition metal ions and the electrons. The cation- $\pi$  interaction occurs between cations and  $sp^2$  clusters. The coexistence of  $sp^2$ - $sp^3$  regions in the stacked lamellar structure creates numerous nanocapillaries. The presence of nanocapillaries shows significant molecular sieving effects (Figure 2). These different cross-linking effects make GO a useful tool for membrane separation and energy generation.

The surface properties of the reassembled GO nanosheets determine the ionic transport behaviors of the GO-based membranes. The surface-charge-governed ion transportation preferentially permeates the counterions and excludes the co-ions.<sup>24</sup> For example, the small protons

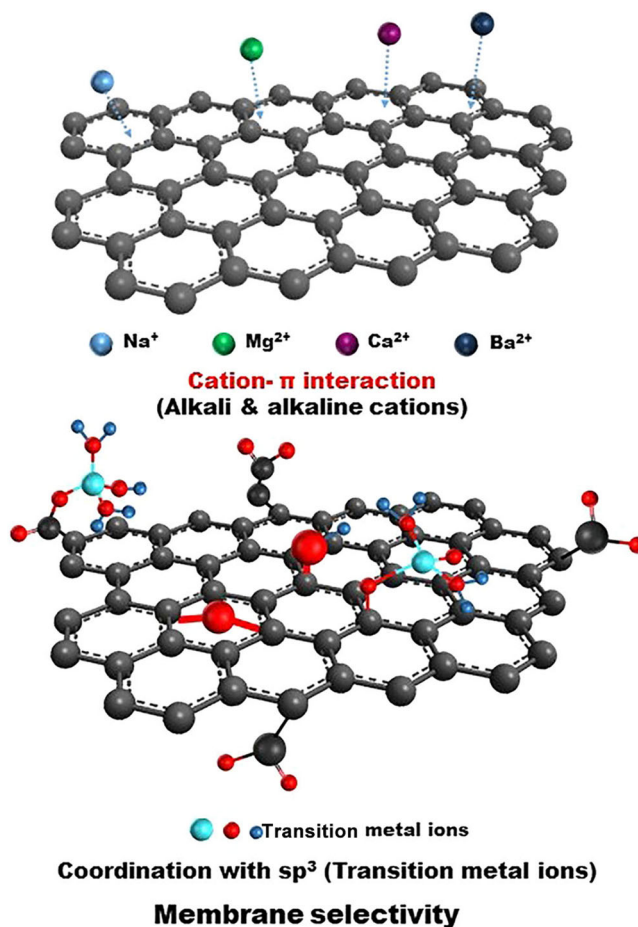


**FIGURE 2** Cation- $\pi$  interactions and  $sp^3$  coordination of graphene-containing systems.

attract negatively charged, oxygen-containing groups. The networks then deliver the protons rapidly along with the water layers. The strong electrostatic repulsion between these ions and the anions on the GO limits the transportation of the co-ions ( $Cl^-$  or  $SO_4^{2-}$ ). Mobile cations in the solution migrate through the nanochannels in a nearly unipolar way. This typically occurs when driven by a hydraulic flow (Figure 3).<sup>25</sup>

Covalent or noncovalent modifications on the GO structure can improve the performance of GO.<sup>26</sup> This includes covalent functionalization via the  $sp^2$  structure with defects, noncovalent modification with the introduction of new chemical groups by polymer wrapping,  $\pi$ - $\pi$  interactions, hydrogen bonding, electrostatic interaction, and van der Waals forces.<sup>27</sup> It provides both a physical possibility (such as the interlayer spaces to control the ion transport) and a chemical possibility (such as the modification of oxygen-containing groups via chemical reactions including isocyanate, carboxylic acylation, epoxy ring opening, and diazotization).<sup>28</sup> In addition, multivalent ions can modify the charges within the pores, and the manufacturing conditions may influence ionic selectivity.

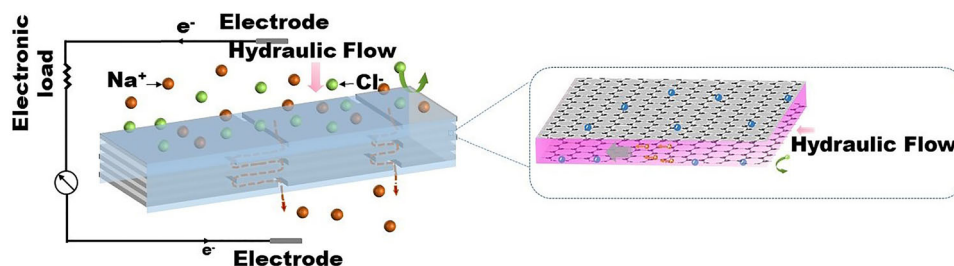


FIGURE 3 The GO membrane works as a charged filter. The transport of counterions (+) occurs while the migration of co-ions (–) does not. Reproduced with permission: Copyright 2013, Wiley-VCH.<sup>25</sup>

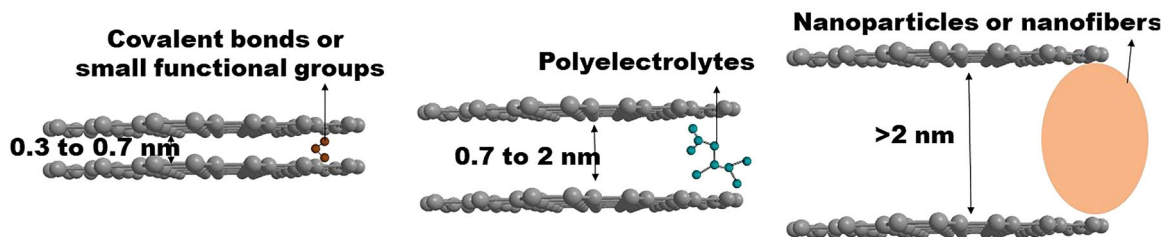


FIGURE 4 Adjusting the nanochannel size changes the interlayer spacing of a GO membrane. Reproduced with permission: Copyright 2014, Science.<sup>31</sup>

On the other hand, modifications could alter the transport channels. Precisely controlling the transport channels of GO membranes could effectively control the transportation of molecules or ions. Ion sieving in GO membranes is achieved through both size and charge exclusion. Ion sieving by size is controlled by the interlayer distance between the GO flakes. The interlayer spacing and the oxygenated parts can significantly affect the ion transportation of GO membranes.<sup>29</sup> The interlayer channels facilitate selective ionic transport through the matching interlayer spacing and the electrostatic properties of the channel. The approximate interlayer spacing was calculated following the Bragg equation (2) based on the X-ray diffraction results:

$$2d\sin\theta = n\lambda, \quad (2)$$

where  $d$  is the d-spacing of the GO,  $\theta$  is the diffraction angle,  $n$  expresses the diffraction series, and  $\lambda$  is the wavelength of the X-ray beam. The interlayer spacing of a GO membrane averages at 0.8 nm, which increases to 1.4 nm in water, allowing for the transport of most hydrated ions with a diameter less than 1 nm.<sup>30</sup> Deprotonated oxygen functional groups play a crucial role in reducing the energy barrier for cations to enter the GO channels with negatively charged functional groups while simultaneously enhancing the free energy barrier for anions. Consequently, the permeability of anions exhibits a noticeable cutoff at a specific interlayer spacing.

Modulating the interlayer spacing of GO by functionalizing the oxygen-containing groups can enhance a GO membrane's ability to separate targeted ions and molecules (Figure 4).<sup>31</sup> Functionalizing the platelets with atomic species/functional groups that are attracted to the H-bonding network results in a smaller spacing, less than 0.7 nm.<sup>32</sup> This spacing increases after incorporating larger chemical groups or soft polymer chains (e.g., polyelectrolytes) into the GO-spaced nanosheets, facilitated by a subdued van der Waals' force between the spaced layers. This adjustment helps reduce the likelihood of aggregation.<sup>33</sup> Yang et al. demonstrated the capability to fine-tune the interlayer spacing of GO from subnanometers to 10 nm.<sup>34</sup> The intrinsic negative charge inherently present on GO membranes, along with the height of the lamellar nanochannels nearing the Debye screening length, results in surface-charge-governed transport.<sup>35</sup> In a general context, the conductance ( $G$ ) of a single nanofluidic channel encompasses surface conductance (left term) and bulk conductance (right term)<sup>36</sup>

$$G = 2\mu_+\sigma_s(w/l) + z(\mu_+ + \mu_-)cN_A wh/l. \quad (3)$$

Here,  $\mu_+$  and  $\mu_-$  denote the mobility of the cation and anion, respectively,  $\sigma_s$  is the surface charge density,  $c$  represents the concentration of the bulk solution,  $N_A$  is Avogadro's number,  $z$  signifies the elementary charge,  $h$  indicates the interlayer space, and  $w$  and  $l$  correspond to the width and length of the channel, respectively. The

interlayer channels facilitate selective ionic transport through the matching interlayer spacing and the electrostatic properties of the channel. Reducing the spacing to a certain extent increases internal resistance, while increasing it poses a threat to permselectivity. This presents a delicate balance between ion selectivity and permeability, necessitating intricate design guidelines for interlayer spacing. For example, through a vapor diffusion reaction of GO with ethylenediamine, the interlayer channel gradually opens up as the reaction time increases. The output power density reaches a peak of  $5.32 \text{ W m}^{-2}$  when the reaction time is extended to 10 min.<sup>37</sup>

In practical application, antifouling determines a membrane's usefulness in aqueous and salty solutions.<sup>38</sup> Membranes with nanoscale pores can experience blockage with impurities, such as biological pollutants, and organic sulfates. This causes a significant decrease in the pressure and the power density. The hydrophilicity or interfacial energy determines the antifouling properties of a membrane.<sup>39</sup> A surface adsorption property depends on its hydrophilicity. Thus, enhancing a membrane's hydrophilicity increases its antifouling properties.<sup>40</sup> High hydrophilicity gives rise to a high water flow. This results in low interfacial energy between GO's surface and water.<sup>41</sup> More hydrophilic surfaces with negative zeta potential could enhance the fouling resistance. For example, GO can improve the flux and antifouling properties of hydrophobic membranes. GO can thus prevent the membrane from biofouling by generating an electrostatic repulsion against microorganism deposition.<sup>42</sup> GO can generate oxidative stress by producing reactive oxygen species. This leads to the reduction in metabolic activities and the death of bacterial cells.

### 3 | GO-POLYMER COMPOSITE MEMBRANES FOR RECTIFIERS

Traditional RED membranes have suffered from poor energy conversion efficiency and low power density due to high ionic transport resistance in their porous channels.<sup>43</sup>

Ionic diodes are fluidic devices that demonstrate ion-rectifying properties, characterized by asymmetric current–voltage ( $I$ – $V$ ) curves. These curves show that the current for one voltage polarity surpasses that for the opposite polarity.<sup>44</sup> This diode-like behavior suggests a preferential direction for ion flow.

Rectifiers might function similarly to the electronic rectification seen in semiconductor p–n junctions, capable of realizing ionic rectification. They conduct ionic current preferentially in one direction and display a nonlinear electric response to the voltage drop. Such

rectifiers, functioning as “fluidic Shockley diodes,” inhibit the flow of reverse current. This prevents the dissipation of osmotic energy as Joule heat during nanochannel transport, thereby enhancing blue energy conversion under a salinity gradient.<sup>24</sup>

As a 2D material, nanofluidic GO is a well-known electrical insulator, as previously noted, which reduces the risk of short circuits and exhibits excellent ionic conductivity. However, the laminated structures within GO membranes accelerate concentration polarization in low-concentration solutions during ionic transport processes, interrupting continuous osmotic power generation. To enhance power density for practical applications, materials with advanced structures that can address the tradeoff between permselectivity and ion conductivity are required.

The term “membrane permselectivity” denotes the capacity of IEMs to selectively allow counterions to permeate over co-ions. Conductivity in this context is measured as the transport of ions across IEMs, typically in the presence of an electric field. According to the Poisson–Boltzmann equation and Debye length, selectivity increases with smaller pore sizes and longer channel lengths.<sup>45</sup> Correspondingly, the ion diffusion coefficient ( $D$ ) decreases, leading to lower conductivity ( $\sigma$ ), as described by the Nernst–Einstein (N–E) Equation (4)<sup>46</sup>

$$\sigma = CF^2 v z^2 D / RT. \quad (4)$$

This formulation resulted in the formation of an ion-depleted region on the single wall, introducing new resistance into the system. The ions transported back to the ion-depleted region decrease selectivity. Addressing this challenge involves ion-exchange capacity and uniport of ions. Higher charge density enhances co-ion exclusion, facilitating the transport of counterions. Simultaneously, to maintain electroneutrality, increasing counterions within the membrane matrix is essential. Mobile ions within the matrix lead to greater ion fluxes, improving conductivity. Uniport of ions through membranes, akin to the cell membrane in biological mechanisms, is desirable to balance and offset the trade-off between permselectivity and conductivity. This can be achieved through well-designed asymmetric nanochannel membranes (ANMs), characterized by asymmetric surface charge/or geometry in their nanopores. ANMs enhance the osmotic energy conversion process through efficient ion-selective transport or uniport of, driven by an ionic diode effect.<sup>47</sup> This ionic diode behavior prevents potential power dissipation within the nanochannels, creating an ion accumulation or depletion zone at the boundary depending on a voltage bias.<sup>48</sup> In the case of asymmetric membranes with a dipolar charge distribution, the concentration of counterions at the

channel outlet is much lower than the bulk value, indicating significant counterion depletion. Consequently, concentration polarization at the low-concentration side is effectively suppressed, contributing to the high power density of asymmetric-shaped nanochannel membranes.<sup>49</sup> The power density of the resistor in the circuit can be calculated using Equation (5)

$$P = I_{\text{osmosis}}^2 R_L, \quad (5)$$

where  $I_{\text{osmosis}}$  is the measured current density and  $R_L$  is the loading resistor. Increasing the load resistance reduces current density, and output power reaches a maximum when the load resistance equals the internal resistance of the membrane. The lower resistance of the membranes, thanks to the blockage of reverse current under a reverse bias, leads to higher output power density.

Charge density plays a crucial role in determining a membrane's rectification behavior.<sup>50</sup> Rectification occurs when the concentration of counterions exceeds that of co-ions, causing the charge density to be determined by the nanochannel region. Rectified ion transport results from the asymmetric distribution of electric double layers (EDLs). This results in a diode-like current–voltage ( $I$ – $V$ ) curve and establishes a bipolar ionic diode.<sup>27</sup> Increasing surface charges improves permselectivity and rectification ratios. Reports suggest that prestacked GO laminate functionalized with ionizable functional groups exhibited outstanding salt rejection and ultrahigh water permeance in nanofiltration processes.<sup>22</sup>

Diverse interactions among anions, cations, and charged GO layers lead to cation-controlled permeation. GO films with densely packed nanochannels enable the high flux of molecular/ionic transport.<sup>51</sup> Geometric symmetry allows them to exhibit ion current rectification behavior, with a unique susceptibility to counterion trapping and release. Cation mobility within GO determines ionic resistance in the accumulation/depletion area and leads to selective ionic transport with an ionic current rectification effect. It has been demonstrated that increasing system asymmetry could display nonlinear  $I$ – $V$  characteristics and ion current rectification in GO nanofluidic devices.<sup>51</sup> By modulating the thickness geometry of a GO membrane, directional preferential diffusion becomes controllable from the thick side toward the thin side through a thickness gradient.<sup>52</sup>

The ionization status undergoes significant changes with variations in a solution's pH, resulting in corresponding redistributions of charges on the surface of GO nanochannels.<sup>53</sup> Surface charges attract oppositely charged ions in the solution, creating an EDL to

maintain electrical neutrality. The surface charge density and electrolyte concentration affect the thickness of the EDL, typically in the range of 1–30 nm. An increase in the concentration of hydrochloric acid induces powerful changes, potentially leading to accumulation and depletion effects in the microhole region.<sup>48</sup> Decreasing pH values effectively increases co-ionic permeability through GO nanochannels, reducing the difference in co-ion/counterion current and resulting in a weak rectification effect. Protonation of groups like carboxylic acid weakens electrostatic repulsion by reducing the interlayer spacing of GO membranes, leading to increased rejection rates.<sup>46</sup> It has been reported that the interlayer spacing ( $d$ ) dramatically reduces from 14.7 to 13.4 Å with increasing acidity from pH = 7 to 3,<sup>54</sup> as positively charged ions suppress the EDL of GO.<sup>55</sup> As pH continuously increases, both repulsion forces between GO sheets and ionic screening effects are enhanced. The former increases interlayer spacing, while the latter leads to molecule rejection.<sup>56</sup> When pH falls within the range of 6–8, the ionic screening effect is negligible compared to the electrical repulsion force due to the low ion concentration. As a result, the flux and rejection rate remain relatively unchanged due to stable nanochannels. However, as pH exceeds 9, the ionic screening effect predominates, causing interspacing to shrink and enhancing the rejection rate.<sup>57</sup>

GO nanosheets can optimize the performance of compound asymmetric ionic diode devices<sup>52</sup> and enable these devices to respond to stimuli in RED systems (Figure 5). Asymmetric proton transport phenomena through a GO heterojunction membrane (positively charged GO and negatively charged GO) result in a preferred diffusive and streaming proton current.<sup>62</sup> Table 1 presents the parameters and performance of various types of GO-based membranes.

The inclusion of GO coated on conical nanoporous polyimide (PI) significantly improved the ionic rectification ratio, increasing it from 17 (for PI without GO) to 63.<sup>58</sup> In the case of the GO/GO-polyetherimide (PEI) membrane with charge asymmetry, a rectification factor of 50 was achieved, driven by ion accumulation and depletion in the junction region. This value further increased to 108 by adjusting the pH values of the electrolytes.<sup>59</sup> A GO/poly(ethylene terephthalate) composite was found to absorb substantial amounts of cations, functioning as a cation source to enhance ion selectivity, resulting in a remarkable ion rectification ratio of 238.<sup>60</sup> Visible light with a wavelength of 420 nm, at various power intensities, offers a precise and robust means of modulating smart positive charge-modified anodized aluminum oxide/GO-MOF devices.<sup>61</sup>

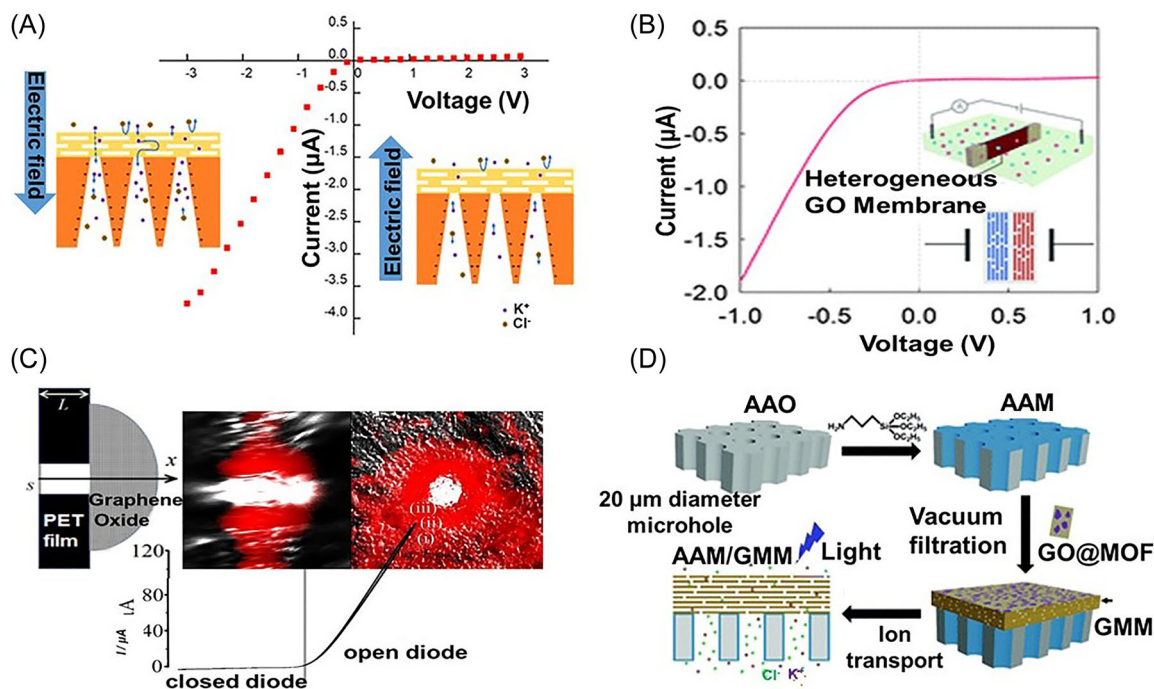


**FIGURE 5** The figure illustrates various methods for regulating ion transport using graphene oxide membranes. (A) A composite of GO membrane and conical nanoporous polyimide for ion transport regulation. Reproduced with permission: Copyright 2021, American Chemical Society.<sup>58</sup> (B) A positively charged polyetherimide (PEI)-grafted GO laminate for rectified ion transport. Reproduced with permission: Copyright 2019, The Royal Society of Chemistry.<sup>59</sup> (C) A cationic rectifier utilizing a GO-covered microhole. Reproduced with permission: Copyright 2019, American Chemical Society.<sup>60</sup> (D) An optoelectronic modulation of ionic conductance and rectification achieved through a heterogeneous 1D/2D nanofluidic membrane. Reproduced with permission: Copyright 2020, The Royal Society of Chemistry.<sup>61</sup>

**TABLE 1** Properties and performance of GO-based nanofluidic rectifiers.

Material	Thickness ( $\mu\text{m}$ )	Electrolyte	Rectification ratio	Reference
GO/PET	12	0.01 M KCl	238	[53]
GO-PI	~13	5 mM KCl	63	[59]
PEI-GO	~6	1 mM KCl	50	[60]
GO/PET	6	0.01 M HCl	28	[61]
GO@MOF/AAO	~30	0.01 M KCl	~2.7	[62]
GO/rGO device	~200	Ionic liquids Ionogels	~6	[64]
PAA/GO	~40	1 mM KCl	4	[65]
GO/RGO	30–50	0.01 M NaCl	20	[66]

Abbreviations: AAO, anodic aluminum oxide; GO, graphene oxide; MOF, metal-organic framework; PAA, porous anodic alumina; PEI, polyetherimide; PET, poly(ethylene terephthalate); PI, polyimide; rGO, reduced GO.

## 4 | GO-BASED MEMBRANE FOR RED POWER GENERATION SYSTEM

During the conversion process, counterions accumulate in the diffusion boundary layers, which screen selectivity,<sup>24</sup> thus impeding effective ion transportation and reducing

energy conversion efficiency. However, membranes with asymmetric charges can prevent counterion accumulation and function as diodes, eliminating polarization and power dissipation. In rectifiers, these membranes effectively convert energy and are ideal for RED systems. As discussed earlier, permselectivity and conductivity are crucial for energy conversion, with abundant surface

charge, suitable pore size, and an asymmetric ratio being key factors in designing asymmetric membranes.

GO materials, with their adjustable properties, offer substantial opportunities for advancing energy-transforming devices (Figure 6). The performance of these devices indicates a promising energy density suitable for industrial development needs. From the aspects of fundamental transport mechanisms, the fundamental approach lies in overcoming the trade-off between ion permeability and selectivity.

Unidirectional interlayer paths within vertically transported 2D nanosheet structures enable ultrafast ion migration, presenting an encouraging avenue. By

manipulating the orientation of GO nanosheets, a vertically transported GO (V-GO) membrane achieved an impressive output power density of  $10.6 \text{ W m}^{-2}$  when exposed to artificial seawater and river water.<sup>66</sup> Notably, this value significantly surpasses that of most commercial IEMs.<sup>69</sup> Within these unidirectional interlayer paths, ions permeate along the lamination direction, resulting in exceptional ion permeability performance. The ion penetration within V-GO membranes facilitates a short migration distance, efficiently promoting the rate of ionic transport. Moreover, the distinctive vertical geometry reduces the entrance barrier, providing rapid and efficient access to the internal channel. The charge density of GO

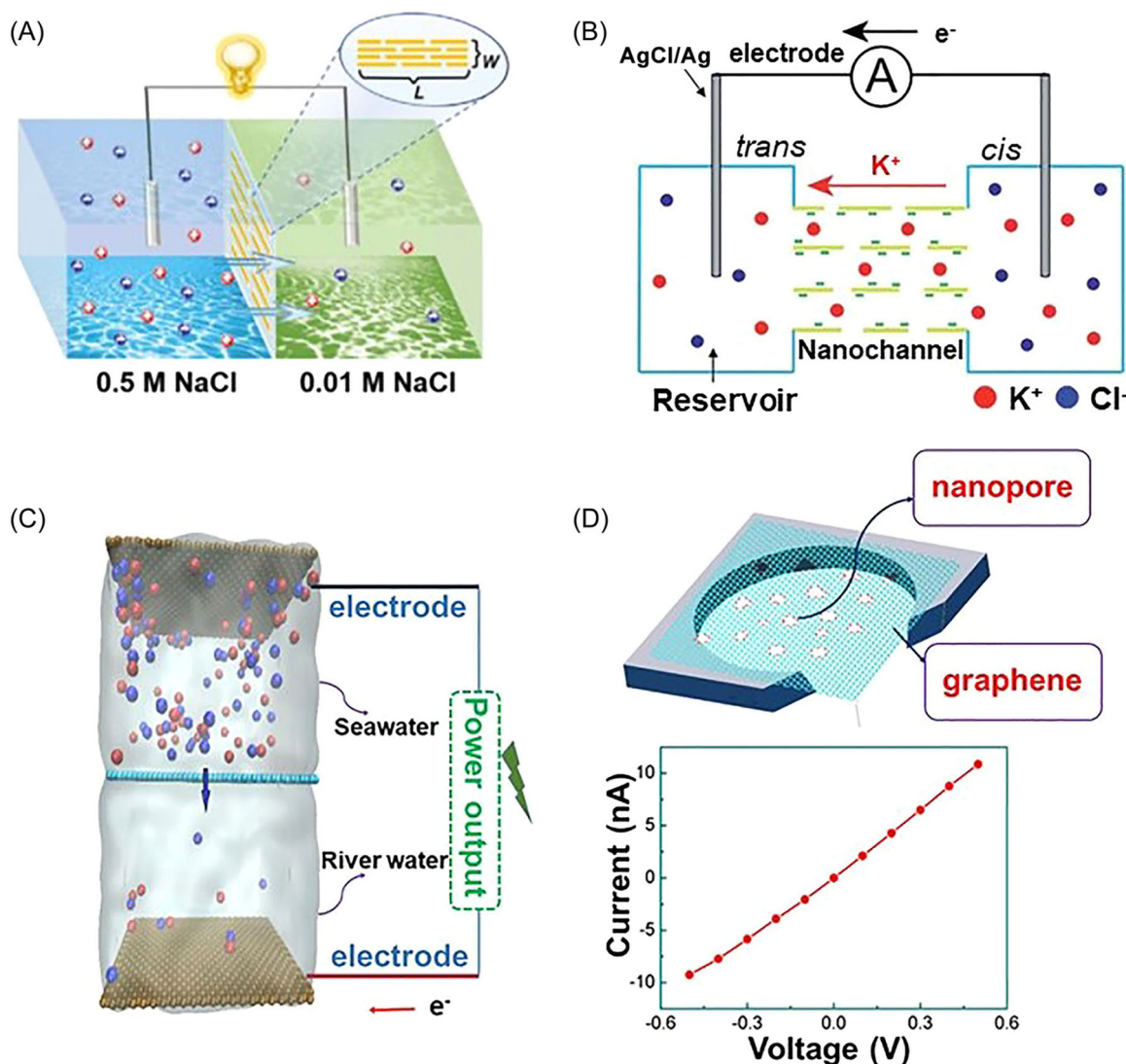


**FIGURE 6** GO materials for the development of energy-transforming devices. (A) Diagram of a system converting salinity gradient to electricity. Reproduced with permission: Copyright 2020, Wiley-VCH.<sup>66</sup> (B) Schematic illustration of the salinity-gradient power generation system with graphene quantum dots/graphene fiber nanochannels. Reproduced with permission: Copyright 2019, The Royal Society of Chemistry.<sup>67</sup> (C) Nanoporous graphene sheet on a hole-punched poly(ethylene terephthalate) (PET) foil ( $1.5 \mu\text{m}^2$  hole) for power generation. (D)  $I$ - $V$  characteristic of nanoporous graphene measured in 1 M KCl electrolyte. Reproduced with permission: Copyright 2019, Elsevier.<sup>68</sup>



can be heightened, along with ion selectivity, through the intercalation of highly charged nanoparticles or by reducing channel dimensions. For example, intercalating graphene quantum dots into the interstitial network of GO sheets within fibers increased the charge density to  $1.12 \text{ mC m}^{-2}$  and raised ion conductance to an average of 21 nS. Consequently, electrical energy generation reached  $0.2 \text{ W m}^{-2}$  at a concentration gradient of 1000.<sup>67</sup> At the pore edge, the charge distribution creates distinct transport barriers for cations and anions, resulting in high ion selectivity. A straightforward ion irradiation perforation approach was employed to fabricate single-layer graphene with subnanometer pores, achieving a record high energy conversion efficiency of nearly 40% and an output power density of  $27 \text{ W m}^{-2}$  at a concentration gradient of 1000.<sup>68</sup>

The intrinsic surface charge density ( $\sim 2 \text{ mC m}^{-2}$ ) of 2D nanochannels is significantly lower than the theoretically expected value ( $300 \text{ mC m}^{-2}$ ) due to atomic structure defects.<sup>70</sup> Enhancing the charge density of 2D GO membranes through hybrid structures or ion selectivity improves ion flux, leading to high energy harvesting performance. GO/polymer heterogeneous membranes exhibit multi-physical-chemical properties that function as navigational switches by altering wettability and surface charge. Charge-density-tunable nanoporous membranes enable concentration-gradient-driven energy harvesting devices to reach a maximum power of  $\sim 0.76 \text{ W m}^{-2}$ .<sup>71</sup> An interfacial superassembly

method involving GO, polyamide, and oxide arrays (anodic aluminum oxide) achieves oriented ion transportation and a power density of up to  $3.73 \text{ W m}^{-2}$ .<sup>72</sup> Polyelectrolyte nanorods/GO membrane systems achieve high osmotic power density and energy conversion efficiency of  $13.12 \text{ W m}^{-2}$  and 35.64%, respectively, owing to high mass transfer resistance and concentration polarization effects.<sup>70</sup>

A 2D GO/three-dimensional (3D) cellulose membrane system for energy harvesting achieves  $0.13 \text{ W m}^{-1}$  for mimicking sea–river water systems and up to  $0.55 \text{ W m}^{-2}$  for a 500-fold salinity gradient.<sup>73</sup> The 3D interface enhances ionic flux, although low ion selectivity limits power density. The introduction of cellulose nanofibers enhances ion selectivity and reduces ion transport energy barriers. Mixing sea and river water results in a power density of  $4.19 \text{ W m}^{-2}$  with improved current.<sup>74</sup> A biomimetic nacre-like GO–silk nanofiber–GO sandwich serves as an osmotic power generator, offering an output power density of  $5.07 \text{ W m}^{-2}$ .<sup>75</sup> While most membranes are fabricated through vacuum filtration for large-scale production, they may display low hydration stability. In addition to GO-based filtration processes, other materials with different processing methods are listed in Table 2. Ionic diode membranes, such as mesoporous carbon/alumina,<sup>69</sup> are manufactured through ion track etching with high production costs. Ionic cable membranes like poly-L-lysine/poly(ethylene terephthalate) (PET)<sup>76</sup> achieve high power density with low ionic resistance but are

**TABLE 2** Properties and performance of nanofluidic materials for the RED salinity power generation system.

Materials	Thickness ( $\mu\text{m}$ )	Rectification ratio	Power ( $\text{W m}^{-2}$ )	Reference
Mesoporous carbon/alumina	64.2	449 (0.1 M KCl)	3.46 (0.5 M/0.01 M NaCl)	[77]
Poly-L-lysine/PET	12	$\sim 25$ (0.1 M KCl)	$\sim 945$ (0.5 M/0.01 M NaCl)	[78]
Polysaccharide hydrogel	50 ~ 300		7.87 (natural water)	[79]
Alumina nanochannel/naion layer	42.9	18.2 (0.01 M KCl)	22.1 (5 M/0.01 M NaCl)	[80]
Polyelectrolyte hydrogel/aramid nanofiber	210	0.01 M KCl (pH $\sim 7$ )	3.9 (0.5 M/0.01 M NaCl)	[81]
Sulfonated polyether ether ketone membrane	27	-	5.8 (0.5 M/0.01 M KCl)	[82]
Block co-polymer/polyethyleneimine	118	17.3 (0.1 M NaCl)	22.4500-fold salinity gradient	[49]
Polyether sulfone/sulfonated polyether sulfone	20	-	2.48 (0.5 M/0.01 M NaCl)	[83]
Silk fibroin	100	21	21.66 (500-fold salinity gradient)/4.06 (0.5 M/0.01 M NaCl)	[84]
MXene/Kevlar nanofiber	2	-	3.7 (0.5 M/0.01 M NaCl)	[85]
Cellulose nanofibers/PET	12	562 (0.01 M KCl)	0.96 (0.5 M/0.01 M NaCl)	[86]

Abbreviation: RED, reverse electrodialysis.

produced through drop processes with nonuniformity. The thickness of the membrane significantly influences energy conversion density and efficiency, showing that energy output inversely correlates with thickness, as demonstrated by high  $945 \text{ W m}^{-2}$  with a minimal thickness of  $12 \mu\text{m}$ .<sup>76</sup> Considering scalability, 3D porous membranes emerge as the ideal choice for creating a simple, high-efficiency harvester with robust output power due to their varied fabrication technologies. Both the structure and surface charge properties critically impact ion transport and power generation.<sup>48</sup> By finely balancing permselectivity and ionic conductivity, power generation can reach optimal levels.

The interaction between GO and water molecules can efficiently generate electrical power. This power system relies on the gradient of oxygen-containing groups, which, with the assistance of adsorbed moisture, induces periodic electric output in response to changes in humidity levels. This property holds great promise for future portable electronics, enabling them to power devices and charge energy storage units (Figure 7).<sup>85–88,90,91</sup> By forming a GO film with an

oxygen-containing group gradient, an energy-harvesting moisture/electric field device was created. This device exhibits remarkable sensitivity to moisture variations (relative humidity variation of less than 5%) and boasts a high energy conversion efficiency of approximately 62% and a power density of around  $4.2 \text{ mW m}^{-2}$  when utilizing tidal moisture as a source.<sup>89</sup> By converting the respiratory moisture expelled by individuals into electric power, this device can ingeniously monitor the body's conditions in real time without the need for an external power supply. It holds significant potential for efficient energy generation and sensing applications.

## 5 | INSIGHTS AND CONCLUSIONS

With the advancements in nanotechnology and biomedical sciences, implantable biomedical devices have become increasingly prevalent. Among the various power sources, the RED system stands out as a versatile option for integration with living organisms, as it mitigates compatibility issues between soft tissues and solid

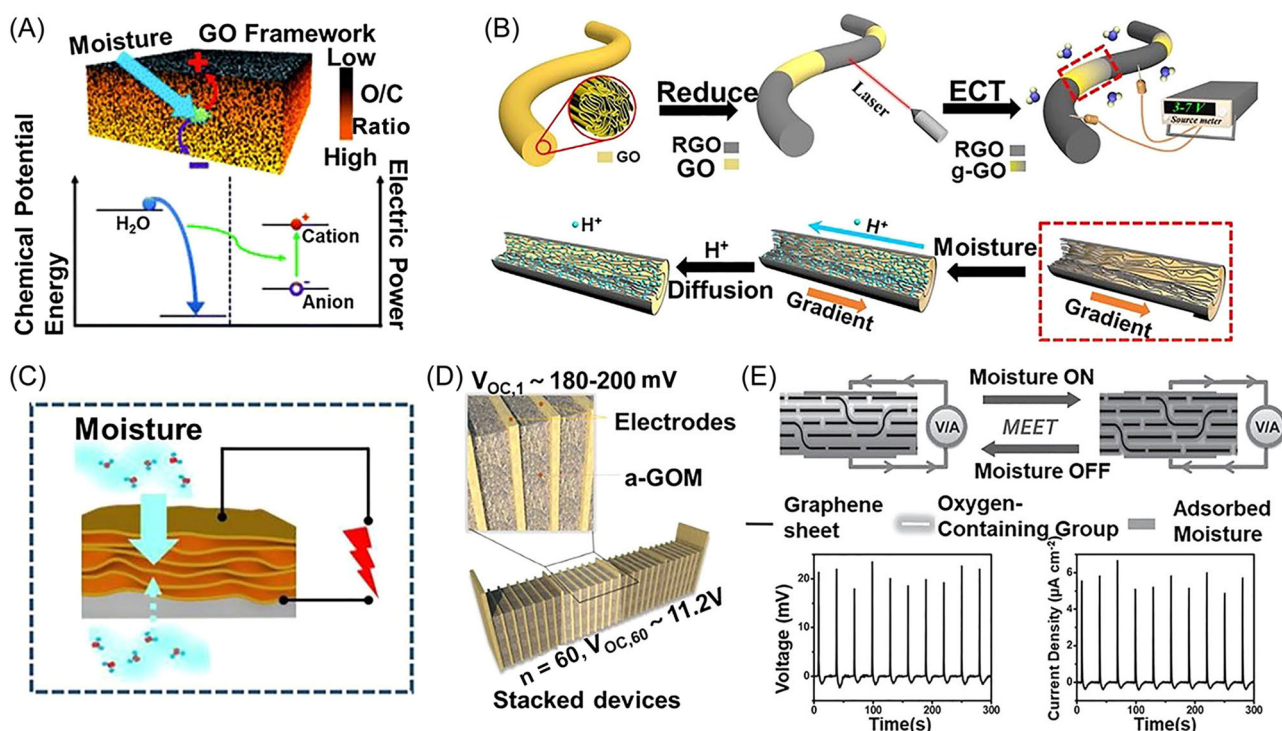


**FIGURE 7** The interaction between GO and water molecules for power devices. (A) An asymmetric 3D GO framework in a chemical potential energy harvesting system. Reproduced with permission: Copyright 2016, The Royal Society of Chemistry.<sup>85</sup> (B) A schematic illustrating the fabrication of a graphene fiber power generator. Reproduced with permission: Copyright 2017, Elsevier.<sup>86</sup> (C) A schematic depicting the generation of an asymmetric moisture stimulus-induced potential. Reproduced with permission: Copyright 2018, The Royal Society of Chemistry.<sup>87</sup> (D) A schematic illustration of a stacked device composed of arranged oxygen-rich GO membranes and electrodes alternately. Each unit can generate a voltage of 180–205 mV. Reproduced with permission: Copyright 2018, The Royal Society of Chemistry.<sup>88</sup> (E) An example of the operation of the GO-based moisture–electric energy transformation process. Reproduced with permission: Copyright 2015, Wiley-VCH.<sup>89</sup>

material surfaces. Similar to biological systems that leverage salt gradients between semipermeable membranes as energy sources, the prospect of biocompatible devices capable of converting the body's chemical energy into electricity holds great promise.<sup>92</sup> Recent research has centered on intelligent energy generation and storage systems that can interact with and respond to external stimuli.<sup>93</sup> RED technology harnesses water-based ion gradient compartments bounded by a repeating sequence of cation- and anion-selective biocompatible membranes. An intriguing recent development is the miniaturized RED device (depicted in Figure 8), which comprises a subcutaneously implanted silk fibroin-based IEM in a Sprague–Dawley rat's back region, yielding an open-circuit voltage of 0.441 V.<sup>94</sup> It has also been reported that a biocompatible droplet device, based on a salinity gradient, can modulate neuronal network activities in neural microtissues.<sup>95</sup> Cytocompatible polypyrrole

membranes have shown the capability to generate salinity power, opening doors to biomimetic applications.<sup>96</sup> Furthermore, a mesoporous carbon-silica/anodized aluminum nanofluidic device has emerged, offering enhanced permselectivity and serving as a temperature- and pH-regulated energy generator, achieving a maximum power density of  $5.04 \text{ W m}^{-2}$ .<sup>97</sup> This breakthrough hints at the potential of RED technology in sensory systems with temperature- and pH-regulated energy conversion.

While these materials can serve as ion-selective membranes in bio-RED systems, their limited smart response properties hinder their bioelectrogenic potential. Here, 2D graphene materials take the spotlight, offering tuneable interlayer spaces ideal for fast and selective nanochannels for ion transport.<sup>98</sup> The presence of hydroxyl and carboxyl groups introduces novel possibilities for direct interaction with biological

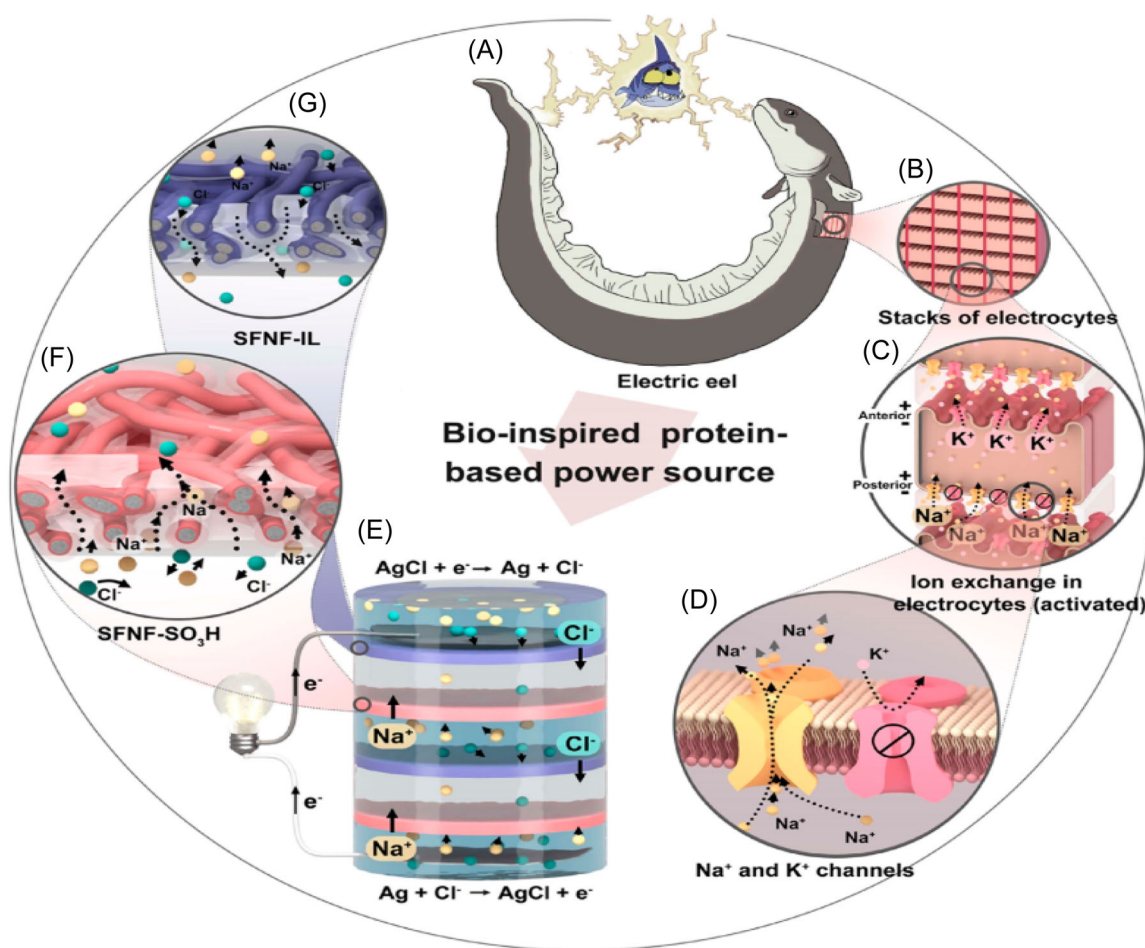


**FIGURE 8** Schematic of an electric eel-inspired cell featuring protein-based ion-exchange membranes. (A) Electric eels stunning their prey. (B) Stacks of electrolytes bound by insulating tissue. (C) Ion exchange across the anterior and posterior plasma membranes in the activated state. (D) Activated  $\text{Na}^+$  and closed  $\text{K}^+$  channels. (E) Working principle of RED devices. (F) Cation selectivity of negatively charged protein-based ion-exchange membranes. (G) Anion selectivity of positively charged membranes. Copyright 2021, American Chemical Society.<sup>94</sup>

molecules. For instance, GO-biomimetic DNA nanochannels can function as ionic gates, switching between ON/OFF states when exposed to visible and ultraviolet light.<sup>99</sup> Responsive molecules can be incorporated into stimulus-gated nanochannels, enabling adjustments in response to pH, light, temperature, and pressure changes.<sup>100</sup> GO-based membranes might achieve exceptional ion selectivity, closely resembling biological ion channels.<sup>101</sup> This promising application of GO for biomimetic recognition of selective ion transport and its synergistic use with biomimetic strategies demonstrate the potential of these innovative features for adaptive power generation systems, potentially underreported in other studies. These innovative features allow for adaptive power generation systems using well-designed GO membrane technologies that may be underreported elsewhere.

The IEM plays a pivotal role in determining the energy generation performance of an RED system. By chemically modifying GO with functional groups or molecules, it is possible to alter the surface properties of the channel wall and control mass and charge transport behaviors. By chemically modifying GO with functional groups or molecules, one can change the surface properties of the channel wall and control mass and charge transport behaviors. GO has seen extensive research in the fields of membrane pervaporation related to salinity,<sup>102</sup> salt stress reduction in plants,<sup>103</sup> and anticorrosion in high-salinity environments.<sup>104</sup> This tunability holds immense potential for energy applications. This work has highlighted both the challenges and opportunities associated with GO-based membranes, shedding light on their efficacy in membrane separations, energy generation, nanofluidic rectifiers, and energy harvesting systems.

Nonetheless, several critical challenges remain in this field. Despite the encouraging aspects of 2D GO materials, their poor stability in aqueous environments poses a significant challenge to their practical use in salinity energy harvesting. While most authors focus on the power density of an RED stack,<sup>105</sup> it is crucial to recognize the interplay between power density and energy efficiency, which often conflict. In practical commercial applications, both power density and efficiency, measuring the energy harvested compared to the available energy in feed waters, are of paramount importance. Future research should systematically investigate power density, thermodynamic efficiency, and energy efficiency. Additionally, enhancing the integrity and mechanical properties of GO-based membranes, along with exploring solvent environments beyond water, will expand their practical utility in salinity energy harvesting.

## AUTHOR CONTRIBUTIONS

Changchun Yu, Shulei Chou, and Yong Liu conceived the idea and guided the review. Changchun Yu drafted the original manuscript. Yiming Xiang and Yandi Zhou assisted in literature search and manuscript preparation. Tom Lawson and Pingan Song carried out the concepts, design, and manuscript editing. Shulei Chou and Yong Liu supervised the manuscript.

## ACKNOWLEDGMENTS

We gratefully acknowledge the generous support provided by the following organizations: Natural Science Foundation of Zhejiang Province (LQ21H180012), Key Research and Development Program of Zhejiang Province (2021C04019), and National Natural Science Foundation of China (U20A20338). The valuable consultation and instrument support from the Scientific Research Centre of Wenzhou Medical University is acknowledged.

## CONFLICT OF INTEREST STATEMENT

The authors declare that there are no conflict of interests.

## ORCID

Yong Liu  <https://orcid.org/0000-0001-6932-583X>

## REFERENCES

- Zhou Y, Jiang L. Bioinspired nanoporous membrane for salinity gradient energy harvesting. *Joule*. 2020;4(11):2244-2248.
- Jianbo L, Chen Z, Kai L, Li Y, Xiangqiang K. Experimental study on salinity gradient energy recovery from desalination seawater based on RED. *Energy Convers Manag*. 2021;244:114475.
- Tong X, Liu S, Crittenden J, Chen Y. Nanofluidic membranes to address the challenges of salinity gradient power harvesting. *ACS Nano*. 2021;15(4):5838-5860.
- Macha M, Marion S, Nandigana VVR, Radenovic A. 2D materials as an emerging platform for nanopore-based power generation. *Nat Rev Mater*. 2019;4(9):588-605.
- Moya AA. Numerical simulation of ionic transport processes through bilayer ion-exchange membranes in reverse electro-dialysis stacks. *J Membr Sci*. 2017;524:400-408.
- Kotoka F, Merino-Garcia I, Velizarov S. Surface modifications of anion exchange membranes for an improved reverse electro-dialysis process performance: a review. *Membranes*. 2020;10(8):160.
- Santoro S, Tufa RA, Avci AH, Fontananova E, Di Profio G, Curcio E. Fouling propensity in reverse electro-dialysis operated with hypersaline brine. *Energy*. 2021;228:120563.
- Bodzek M, Konieczny K, Kwiecińska-Mydlak A. Nanotechnology in water and wastewater treatment. Graphene—the nanomaterial for next generation of semipermeable membranes. *Crit Rev Environ Sci Technol*. 2020;50(15):1515-1579.
- Liu X, He M, Calvani D, et al. Power generation by reverse electro-dialysis in a single-layer nanoporous membrane made from core-rim polycyclic aromatic hydrocarbons. *Nat Nanotechnol*. 2020;15(4):307-312.

10. Kamcev J. Reformulating the permselectivity-conductivity tradeoff relation in ion-exchange membranes. *J Polym Sci.* 2021;59(21):2510-2520.
11. Post JW, Hamelers HVM, Buisman CJN. Energy recovery from controlled mixing salt and fresh water with a reverse electrodialysis system. *Environ Sci Technol.* 2008;42(15):5785-5790.
12. Mei Y, Tang CY. Recent developments and future perspectives of reverse electrodialysis technology: a review. *Desalination.* 2018;425:156-174.
13. Zhang B, Gao H, Chen Y. Enhanced ionic conductivity and power generation using ion-exchange resin beads in a reverse-electrodialysis stack. *Environ Sci Technol.* 2015;49(24):14717-14724.
14. Liu Y-C, Yeh L-H, Zheng M-J, Wu KCW. Highly selective and high-performance osmotic power generators in subnanochannel membranes enabled by metal-organic frameworks. *Sci Adv.* 2021;7(10):eabe9924.
15. Lee S, Kim H, Kim D-K. Power generation from concentration gradient by reverse electrodialysis in dense silica membranes for microfluidic and nanofluidic systems. *Energies.* 2016;9(1):49.
16. Stucki M, Loepfe M, Stark WJ. Porous polymer membranes by hard templating—a review. *Adv Eng Mater.* 2018;20(1):1700611.
17. Zazyev OV, Chen YP. Polycrystalline graphene and other two-dimensional materials. *Nat Nanotechnol.* 2014;9(10):755-767.
18. Huang X, Yin Z, Wu S, et al. Graphene-based materials: synthesis, characterization, properties, and applications. *Small.* 2011;7(14):1876-1902.
19. Li Y, Shi Y, Wang H, et al. Recent advances in carbon-based materials for solar-driven interfacial photothermal conversion water evaporation: assemblies, structures, applications, and prospective. *Carbon Energy.* 2023;5(11):e331.
20. Su P, Iwase K, Nakanishi S, Hashimoto K, Kamiya K. Nickel-nitrogen-modified graphene: an efficient electrocatalyst for the reduction of carbon dioxide to carbon monoxide. *Small.* 2016;12(44):6083-6089.
21. Xin W, Jiang L, Wen L. Two-dimensional nanofluidic membranes toward harvesting salinity gradient power. *Acc Chem Res.* 2021;54(22):4154-4165.
22. Liu F, Wang C, Sui X, et al. Synthesis of graphene materials by electrochemical exfoliation: recent progress and future potential. *Carbon Energy.* 2019;1(2):173-199.
23. Choi S, Kim C, Suh JM, Jang HW. Reduced graphene oxide-based materials for electrochemical energy conversion reactions. *Carbon Energy.* 2019;1(1):85-108.
24. Zhang Z, Wen L, Jiang L. Nanofluidics for osmotic energy conversion. *Nat Rev Mater.* 2021;6(7):622-639.
25. Guo W, Cheng C, Wu Y, et al. Bio-inspired two-dimensional nanofluidic generators based on a layered graphene hydrogel membrane. *Adv Mater.* 2013;25(42):6064-6068.
26. Dreyer DR, Todd AD, Bielawski CW. Harnessing the chemistry of graphene oxide. *Chem Soc Rev.* 2014;43(15):5288-5301.
27. Georgakilas V, Tiwari JN, Kemp KC, et al. Noncovalent functionalization of graphene and graphene oxide for energy materials, biosensing, catalytic, and biomedical applications. *Chem Rev.* 2016;116(9):5464-5519.
28. Chen D, Feng H, Li J. Graphene oxide: preparation, functionalization, and electrochemical applications. *Chem Rev.* 2012;112(11):6027-6053.
29. Abraham J, Vasu KS, Williams CD, et al. Tunable sieving of ions using graphene oxide membranes. *Nat Nanotechnol.* 2017;12(6):546-550.
30. Joshi RK, Carbone P, Wang FC, et al. Precise and ultrafast molecular sieving through graphene oxide membranes. *Science.* 2014;343(6172):752-754.
31. Mi B. Graphene oxide membranes for ionic and molecular sieving. *Science.* 2014; 343(6172):740-742.
32. Medhekar NV, Ramasubramaniam A, Ruoff RS, Shenoy VB. Hydrogen bond networks in graphene oxide composite paper: structure and mechanical properties. *ACS Nano.* 2010;4(4):2300-2306.
33. Thebo KH, Qian X, Zhang Q, Chen L, Cheng HM, Ren W. Highly stable graphene-oxide-based membranes with superior permeability. *Nat Commun.* 2018;9(1):1486.
34. Yang X, Cheng C, Wang Y, Qiu L, Li D. Liquid-mediated dense integration of graphene materials for compact capacitive energy storage. *Science.* 2013;341(6145):534-537.
35. Aixala-Perello A, Pedico A, Laurenti M, et al. Scalable and highly selective graphene-based ion-exchange membranes with tunable permselectivity. *NPJ 2D Mater Appl.* 2023;7(1):46.
36. Raidongia K, Huang J. Nanofluidic ion transport through reconstructed layered materials. *J Am Chem Soc.* 2012;134(40):16528-16531.
37. Bang KR, Kwon C, Lee H, Kim S, Cho ES. Horizontally asymmetric nanochannels of graphene oxide membranes for efficient osmotic energy harvesting. *ACS Nano.* 2023;17(11):10000-10009.
38. Siria A, Bocquet M-L, Bocquet L. New avenues for the large-scale harvesting of blue energy. *Nat Rev Chem.* 2017;1(11):0091.
39. Tiraferri A, Kang Y, Giannelis EP, Elimelech M. Superhydrophilic thin-film composite forward osmosis membranes for organic fouling control: fouling behavior and antifouling mechanisms. *Environ Sci Technol.* 2012;46(20):11135-11144.
40. Kobayashi M, Terayama Y, Yamaguchi H, et al. Wettability and antifouling behavior on the surfaces of superhydrophilic polymer brushes. *Langmuir.* 2012;28(18):7212-7222.
41. Lee J, Chae H-R, Won YJ, et al. Graphene oxide nanoplatelets composite membrane with hydrophilic and antifouling properties for wastewater treatment. *J Membr Sci.* 2013;448:223-230.
42. Hu M, Zheng S, Mi B. Organic fouling of graphene oxide membranes and its implications for membrane fouling control in engineered osmosis. *Environ Sci Technol.* 2016;50(2):685-693.
43. Sun Y, Dong T, Lu C, et al. Tailoring a poly(ether sulfone) bipolar membrane: osmotic-energy generator with high power density. *Angew Chem Int Ed.* 2020;59(40):17423-17428.
44. Siwy ZS. Ion-current rectification in nanopores and nanotubes with broken symmetry. *Adv Funct Mater.* 2006;16(6):735-746.
45. Hou S, Zhang Q, Zhang Z, et al. Charged porous asymmetric membrane for enhancing salinity gradient energy conversion. *Nano Energy.* 2021;79:105509.
46. Peng J, Zawodzinski TA. Ion transport in phase-separated single ion conductors. *J Membr Sci.* 2018;555:38-44.

47. Li M, Wang C, Liu Z, Song Y, Li D. Ionic diode based on an asymmetric-shaped carbon black nanoparticle membrane. *Adv Funct Mater.* 2021;31(36):2104341.
48. Xiao K, Jiang L, Antonietti M. Ion transport in nanofluidic devices for energy harvesting. *Joule.* 2019;3(10):2364-2380.
49. Li C, Wen L, Sui X, Cheng Y, Gao L, Jiang L. Large-scale, robust mushroom-shaped nanochannel array membrane for ultrahigh osmotic energy conversion. *Sci Adv.* 2021;7(21):eabg2183.
50. Liu J, Kvetny M, Feng J, et al. Surface charge density determination of single conical nanopores based on normalized ion current rectification. *Langmuir.* 2012;28(2):1588-1595.
51. Miansari M, Friend JR, Yeo LY. Enhanced ion current rectification in 2D graphene-based nanofluidic devices. *Adv Sci.* 2015;2(6):1500062.
52. Yang J, Zhang X, Chen F, Jiang L. Geometry modulation of ion diffusion through layered asymmetric graphene oxide membranes. *Chem Commun.* 2019;55(21):3140-3143.
53. Dong Y, Cheng Y, Xu G, et al. Selectively enhanced ion transport in graphene oxide membrane/PET conical nanopore system. *ACS Appl Mater Interfaces.* 2019;11(16):14960-14969.
54. Yeh L-H, Zhang M, Qian S. Ion transport in a pH-regulated nanopore. *Anal Chem.* 2013;85(15):7527-7534.
55. Wu T, Wang Z, Lu Y, et al. Graphene oxide membranes for tunable ion sieving in acidic radioactive waste. *Adv Sci.* 2021;8(7):2002717.
56. Liu G, Ye H, Li A, et al. Graphene oxide for high-efficiency separation membranes: role of electrostatic interactions. *Carbon.* 2016;110:56-61.
57. Huang H, Mao Y, Ying Y, Liu Y, Sun L, Peng X. Salt concentration, pH and pressure controlled separation of small molecules through lamellar graphene oxide membranes. *Chem Commun.* 2013;49(53):5963-5965.
58. Bian Y, Dong Y, Liu J, et al. Graphene oxide membrane/conical nanoporous polyimide composites for regulating ion transport. *ACS Appl Nano Mater.* 2021;4(7):6964-6973.
59. Fei W, Xue M, Qiu H, Guo W. Heterogeneous graphene oxide membrane for rectified ion transport. *Nanoscale.* 2019;11(3):1313-1318.
60. Putra BR, Aoki KJ, Chen J, Marken F. Cationic rectifier based on a graphene oxide-covered microhole: theory and experiment. *Langmuir.* 2019;35(6):2055-2065.
61. Qiao Y, Lu J, Ma W, et al. Optoelectronic modulation of ionic conductance and rectification through a heterogeneous 1D/2D nanofluidic membrane. *Chem Commun.* 2020;56(24):3508-3511.
62. Zhang X, Wen Q, Wang L, et al. Asymmetric electrokinetic proton transport through 2D nanofluidic heterojunctions. *ACS Nano.* 2019;13(4):4238-4245.
63. Wei D, Yang F, Jiang Z, Wang Z. Flexible iontronics based on 2D nanofluidic material. *Nat Commun.* 2022;13(1):4965.
64. Li C, Zhao Y, He L, et al. Mussel-inspired fabrication of porous anodic alumina nanochannels and a graphene oxide interfacial ionic rectification device. *Chem Commun.* 2018;54(25):3122-3125.
65. Martin ST, Neild A, Majumder M. Graphene-based ion rectifier using macroscale geometric asymmetry. *APL Mater.* 2014;2(9):092803.
66. Zhang Z, Shen W, Lin L, et al. Vertically transported graphene oxide for high-performance osmotic energy conversion. *Adv Sci.* 2020;7(12):2000286.
67. Lee KH, Park H, Eom W, Kang DJ, Noh SH, Han TH. Graphene quantum dots/graphene fiber nanochannels for osmotic power generation. *J Mater Chem A.* 2019;7(41):23727-23732.
68. Fu Y, Guo X, Wang Y, Wang X, Xue J. An atomically-thin graphene reverse electro dialysis system for efficient energy harvesting from salinity gradient. *Nano Energy.* 2019;57(7):783-790.
69. Xin W, Xiao H, Kong X-Y, et al. Biomimetic nacre-like silk-crosslinked membranes for osmotic energy harvesting. *ACS Nano.* 2020;14(8):9701-9710.
70. Lee KH, Kang DJ, Eom W, Lee H, Han TH. Holey graphene oxide membranes containing both nanopores and nanochannels for highly efficient harvesting of water evaporation energy. *Chem Eng J.* 2022;430(part 2):132759.
71. Zhu X, Zhou Y, Hao J, et al. A charge-density-tunable three/two-dimensional polymer/graphene oxide heterogeneous nanoporous membrane for ion transport. *ACS Nano.* 2017;11(11):10816-10824.
72. Zhang L, Zhou S, Xie L, et al. Interfacial super-assembly of T-mode janus porous heterochannels from layered graphene and aluminum oxide array for smart oriented ion transportation. *Small.* 2021;17(13):2100141.
73. Jia P, Du X, Chen R, et al. The combination of 2D layered graphene oxide and 3D porous cellulose heterogeneous membranes for nanofluidic osmotic power generation. *Molecules.* 2021;26(17):5343.
74. Wu Y, Xin W, Kong X-Y, et al. Enhanced ion transport by graphene oxide/cellulose nanofibers assembled membranes for high-performance osmotic energy harvesting. *Mater Horizons.* 2020;7(10):2702-2709.
75. Gao J, Guo W, Feng D, Wang H, Zhao D, Jiang L. High-performance ionic diode membrane for salinity gradient power generation. *J Am Chem Soc.* 2014;136(35):12265-12272.
76. Lin C-Y, Combs C, Su Y-S, Yeh LH, Siwy ZS. Rectification of concentration polarization in mesopores leads to high conductance ionic diodes and high performance osmotic power. *J Am Chem Soc.* 2019;141(8):3691-3698.
77. Bian G, Pan N, Luan Z, et al. Anti-swelling gradient polyelectrolyte hydrogel membranes as high-performance osmotic energy generators. *Angew Chem Int Ed.* 2021;60(37):20294-20300.
78. Chang C-W, Chu C-W, Su Y-S, Yeh LH. Space charge enhanced ion transport in heterogeneous polyelectrolyte/alumina nanochannel membranes for high-performance osmotic energy conversion. *J Mater Chem A.* 2022;10(6):2867-2875.
79. Zhang Z, He L, Zhu C, Qian Y, Wen L, Jiang L. Improved osmotic energy conversion in heterogeneous membrane boosted by three-dimensional hydrogel interface. *Nat Commun.* 2020;11(1):875.
80. Zhao Y, Wang J, Kong X-Y, et al. Robust sulfonated poly(ether ether ketone) nanochannels for high-performance osmotic energy conversion. *Natl Sci Rev.* 2020;7(8):1349-1359.
81. Huang X, Zhang Z, Kong X-Y, et al. Engineered PES/SPES nanochannel membrane for salinity gradient power generation. *Nano Energy.* 2019;59:354-362.

82. Chen J, Xin W, Kong X-Y, et al. Ultrathin and robust silk fibroin membrane for high-performance osmotic energy conversion. *ACS Energy Lett.* 2019;5(3):742-748.
83. Zhang Z, Yang S, Zhang P, Zhang J, Chen G, Feng X. Mechanically strong MXene/Kevlar nanofiber composite membranes as high-performance nanofluidic osmotic power generators. *Nat Commun.* 2019;10(1):2920.
84. Xu Y, Song Y, Xu F. TEMPO oxidized cellulose nanofibers-based heterogenous membrane employed for concentration-gradient-driven energy harvesting. *Nano Energy.* 2021;79:105468.
85. Zhao F, Liang Y, Cheng H, Jiang L, Qu L. Highly efficient moisture-enabled electricity generation from graphene oxide frameworks. *Energy Environ Sci.* 2016;9(3):912-916.
86. Liang Y, Zhao F, Cheng Z, et al. Self-powered wearable graphene fiber for information expression. *Nano Energy.* 2017;32:329-335.
87. Liang Y, Zhao F, Cheng Z, et al. Electric power generation via asymmetric moisturizing of graphene oxide for flexible, printable and portable electronics. *Energy Environ Sci.* 2018;11(7):1730-1735.
88. Cheng H, Huang Y, Zhao F, et al. Spontaneous power source in ambient air of a well-directionally reduced graphene oxide bulk. *Energy Environ Sci.* 2018;11(10):2839-2845.
89. Zhao F, Cheng H, Zhang Z, Jiang L, Qu L. Direct power generation from a graphene oxide film under moisture. *Adv Mater.* 2015;27(29):4351-4357.
90. Cheng H, Huang Y, Qu L, Cheng Q, Shi G, Jiang L. Flexible in-plane graphene oxide moisture-electric converter for touchless interactive panel. *Nano Energy.* 2018;45:37-43.
91. Shao C, Gao J, Xu T, et al. Wearable fiberform hygroelectric generator. *Nano Energy.* 2018;53:698-705.
92. Schroeder TBH, Guha A, Lamoureux A, et al. An electric-eel-inspired soft power source from stacked hydrogels. *Nature.* 2017;552(7684):214-218.
93. Ye M, Zhang Z, Zhao Y, Qu L. Graphene platforms for smart energy generation and storage. *Joule.* 2018;2(2):245-268.
94. Lin Z, Meng Z, Miao H, et al. Biomimetic salinity power generation based on silk fibroin ion-exchange membranes. *ACS Nano.* 2021;15(3):5649-5660.
95. Zhang Y, Riexinger J, Yang X, et al. A microscale soft ionic power source modulates neuronal network activity. *Nature.* 2023;620(7976):1001-1006.
96. Yu C, Zhu X, Wang C, et al. A smart cyto-compatible asymmetric polypyrrole membrane for salinity power generation. *Nano Energy.* 2018;53:475-482.
97. Zhou S, Xie L, Li X, et al. Interfacial super-assembly of ordered mesoporous carbon-silica/AAO hybrid membrane with enhanced permselectivity for temperature- and pH-sensitive smart ion transport. *Angew Chem Int Ed.* 2021;60(50):26167-26176.
98. Zhang M, Zhao P, Li P, Ji Y, Liu G, Jin W. Designing biomimic two-dimensional ionic transport channels for efficient ion sieving. *ACS Nano.* 2021;15(3):5209-5220.
99. Shi L, Mu C, Gao T, et al. Rhodopsin-like ionic gate fabricated with graphene oxide and isomeric DNA switch for efficient photocontrol of ion transport. *J Am Chem Soc.* 2019;141(20):8239-8243.
100. Wang J, Fang R, Hou J, et al. Oscillatory reaction induced periodic C-quadruplex DNA gating of artificial ion channels. *ACS Nano.* 2017;11(3):3022-3029.
101. Kim S, Nham J, Jeong YS, et al. Biomimetic selective ion transport through graphene oxide membranes functionalized with ion recognizing peptides. *Chem Mater.* 2015;27(4):1255-1261.
102. Almarzooqi K, Ashrafi M, Kanthan T, Elkamel A, Pope MA. Graphene oxide membranes for high salinity, produced water separation by pervaporation. *Membranes.* 2021;11(7):475.
103. Mahmoud NE, Abdelhameed RM. Superiority of modified graphene oxide for enhancing the growth, yield, and antioxidant potential of pearl millet (*Pennisetum glaucum* L.) under salt stress. *Plant Stress.* 2021;2:100025.
104. Zhu L, Feng C, Cao Y. Corrosion behavior of epoxy composite coatings reinforced with reduced graphene oxide nanosheets in the high salinity environments. *Appl Surf Sci.* 2019;493:889-896.
105. Wang L, Wang Z, Patel SK, Lin S, Elimelech M. Nanopore-based power generation from salinity gradient: why it is not viable. *ACS Nano.* 2021;15(3):4093-4107.

## AUTHOR BIOGRAPHIES



**Dr. Changchun Yu** is an assistant professor at the Laboratory of Novel Optoelectronic Technology for Ophthalmic Devices (NOTOD), School of Ophthalmology & Optometry, School of Biomedical Engineering, Wenzhou Medical University (China). She received her Ph.D. degree from the ARC Centre of Excellence for Electromaterials Science (ACES), University of Wollongong (Australia) in 2019. Her research interests include conducting polymer membrane/hydrogel for ophthalmic diagnostics applications.



**Yiming Xiang** is an undergraduate student from the School of Energy, Quanzhou Vocational and Technical University, China. His research focuses on the development of electroactive nanomaterials for energy conversion and biomedical devices.



**Dr. Tom Lawson** works as a technical member in the School of Chemical Engineering at The University of New South Wales in Sydney, Australia. His research focuses on nanomaterials and their applications in biomedicine and engineering. Tom completed his PhD at Westmead Hospital and Macquarie University. He developed

advanced protocols for *Staphylococcus aureus* characterization. He has made significant contributions to the development of nanomaterials including graphene and metal-organic frameworks for drug delivery biosensors and photothermal therapy. His work includes biomaterials for corneal regeneration and nerve stimulation targeted drug delivery using functionalised nanoparticles and polymers for promoting plant growth.



**Yandi Zhou** is a master student at the Laboratory of Novel Optoelectronic Technology for Ophthalmic Devices (NOTOD), School of Ophthalmology & Optometry, School of Biomedical Engineering, Wenzhou Medical University, China. Her research interest focuses on the novel conductive hydrogels for the regeneration of optic nerve.



**Professor Pingan Song** is a full professor and Australian Research Council (ARC) Future Fellow in the School of Agriculture and Environmental Science and Centre for Future Materials, University of Southern Queensland, Australia. He earned his PhD degree from Zhejiang University (China) in 2009. His research interests involve fire retardants and fire-retardant coatings, sensors, polymers and polymer composites as well as their structure-property correlations.



**Professor Shulei Chou** is a distinguished professor and founding director at the Institute of Carbon Neutralization, College of Chemistry & Materials Engineering, Wenzhou University, China. He obtained his bachelor's degree (1999)

and master's degree (2004) from Nankai University, China. He received his PhD degree from the University of Wollongong (Australia) in 2010. His research interests include energy storage materials for battery applications, especially novel composite materials, new binders, and new electrolytes for Li/Na batteries.



**Professor Yong Liu** is a vice dean of Eye Hospital, School of Ophthalmology and Optometry/School of Biomedical Engineering, Wenzhou Medical University, China. He is the director of the Laboratory of Novel Optoelectronic Technology for Ophthalmic Devices (NOTOD). He received his PhD degree in 2008 from Intelligent Polymer Research Institute (IPRI), University of Wollongong, Australia. After graduation, he was offered as a postdoc scientist in University of Wollongong and University of Dayton (USA). His expertise lies across several fields, including the preparation of photoactive and electroactive nanocomposites for multifunctional applications such as ophthalmic diagnostics, biomedical equipment and electrochemical devices.

**How to cite this article:** Yu C, Xiang Y, Lawson T, et al. Graphene oxide-based nanofluidic membranes for reverse electro dialysis that generate electricity from salinity gradients. *Carbon Energy*. 2025;7:e626. doi:10.1002/cey2.626